

## A Novel Heptagonal Slot Antenna for Ultra Wideband Wireless Communication Applications

Asst. Prof. Dr. Abdulkareem Swadi Abdullah

Lect. Malik Jasim Farhan

Department of Electrical Engineering, College of Engineering, University of Basrah

[drasabdallah@ieee.org](mailto:drasabdallah@ieee.org)

[malik\\_jf1974@yahoo.com](mailto:malik_jf1974@yahoo.com)

### Abstract :

*In this paper, a novel design of heptagonal slot antenna is proposed to be used for ultra wideband (UWB) applications. This antenna has a heptagonal slot with suitable dimensions on the lower side of a dielectric substrate which represents the ground plane, and a symmetrical slant cut ends microstrip line on the upper side of the substrate. In order to cover the entire bandwidth that was specified for UWB applications, a bevel rectangular with rectangular notch cut tuning stub is used to enhance the coupling between the heptagonal slot and the taper microstrip feed line. Several kinds of techniques are used to improve the design of the proposed antenna such as; adjusting the gap between the tuning stub and lower edge of heptagonal slot, adjusting the feed position point of the tuning stub, adjusting the end cut angle of microstrip line and bevel angle of tuning stub. The radiation characteristics of the proposed antenna such as radiation pattern, gain, impedance bandwidth are investigated and found be accepted over the whole operating bandwidth. The proposed antenna also shows a good time domain characteristics and has a linear phase over this band giving less distortion of the received signal.*

*Key words: Heptagonal antenna, slot antenna, printed antenna, UWB antenna, tuning stub.*

### تصميم هوائي سباعي الشق لتطبيقات الاتصالات اللاسلكية فائقة الحزمة

أ.م.د. عبد الكريم سوادى عبدالله

م. مالك جاسم فرحان

قسم الهندسة الكهربائية / كلية الهندسة / جامعة البصرة

### الخلاصة :

في هذا البحث تم تصميم هوائي سباعي الشق والذي اقترح ليعمل في التطبيقات فائقة الحزمة الترددية. هذا الهوائي يتكون من شق سباعي الشكل بابعاد مناسبة يحفر على الطبقة السفلى لمرتكز العازل حيث تمثل هذه الطبقة مستوى الارضى، اما في الطبقة العليا من مرتكز العازل فتحتوي على مغذي شريطي دقيق يحتوي على قطع مانل متناظر عند نهايته ولكي نحصل على استجابة تغطي تطبيقات الحزمة الفائقة بالكامل تم استخدام رقعة مستطيلة الشكل مقطوعة بشكل مانل من الجانبين ومحفورة من المنتصف بحفر مستطيل بابعاد معينة لتكوين العقب الرنان وذلك لتحسين الترابط بين الشق السباعي في الطبقة السفلى والمغذي الشريطي الدقيق في الطبقة العليا.

تم استخدام عدة تقنيات لتحسين تصميم الهوائي المقترح وهذه التقنيات هي: تحديد القيمة الملائمة للفجوة بين العقب الرنان والحافة السفلى للشق السباعي، تحديد نقطة التغذية المناسبة للعقب الرنان، تحديد زاوية القطع المناسبة لنهايتي المغذي الشريطي الدقيق وكذلك تحديد زاوية الميلان المناسبة للعقب الرنان. ان خواص الاشعاع مثل نمط الاشعاع، الكسب و حزمة الممانعة للهوائي المقترح تم فحصها وقد وجدها بانها مناسبة لحزمة العمل. وكذلك قد بين الهوائي المقترح بانه يمتلك خصائص مجال وقت جيدة ويمتلك طور خطي على طول حزمة العمل وهذا يعني انه سوف يستقبل اشارات بتشويبه قليل.

## 1. Introduction

The ultra wideband (UWB) radio system has attracted both industrial and academic communities attentions since the Federal Communication Committee (FCC) approval of frequency band between 3.1GHz to 10.6 GHz for commercial applications in 2002 <sup>[1]</sup>.

Relatively large electric near-fields which are owned by patch antennas make them coupling with nearby objects. In contrary, slot antennas have comparatively large magnetic near-fields that tend not to strongly couple with nearby objects <sup>[2]</sup>. Also, slot antennas have many good merits like light weight, low profile, wide frequency bandwidth and ease of fabrication. Mainly, a slot antenna consists of a slot with certain shape in the lower side of the dielectric substrate that represents the ground plane, and microstrip line with tuning stub are set up on the upper side of the dielectric substrate of the printed-circuit boards (PCBs). In some configurations, the slot in the ground plane, microstrip line and tuning stub are coplanar with each other in the same side of dielectric substrate <sup>[3]</sup>.

There are several kinds of this type of antennas according to the slot shape such as circle, rectangle, triangle, and arc-shape and so on. The feed line of these antennas may be microstrip line, or coplanar waveguide (CPW) <sup>[4-17]</sup>.

In this paper, a novel design of heptagonal slot antenna is proposed for UWB applications. The antenna consists of a heptagonal slot in the ground plane and a bevel rectangular with a rectangular notch cut tuning stub on opposite sides of the substrate. The tuning stub is fed through a  $50\Omega$  microstrip line. The tuning stub is used to increase the matching between the microstrip line in the top of the substrate and the heptagonal slot in the bottom of substrate to widen the operating bandwidth. After setting up the conformation of the antenna, determining the initial parameters and fixing the lower frequency, parametric study is performed to consolidate the calculated parameters. Then several techniques of bandwidth enhancement are applied to broaden the bandwidth and obtain UWB performance. These techniques are: adjusting the distance between the tuning stub and lower edge of heptagonal slot technique, adjusting the slant angle cutting of the end of microstrip line technique, optimum feed point technique and adjusting the bevel angle of tuning stub technique.

## 2. Antenna Design

The proposed slot is configured as heptagonal as shown in **Figure 1** with the FR4 dielectric substrate, which has a relative permittivity  $\epsilon_r = 4.4$  and a thickness  $h = 1.5$  mm.

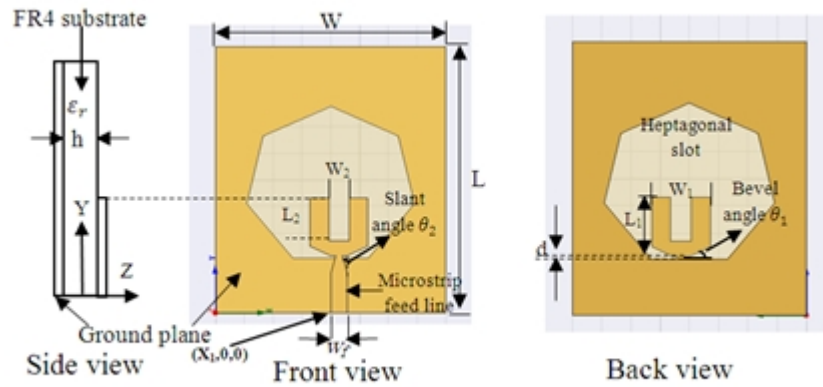


**Fig .(1) The proposed heptagonal slot antenna**

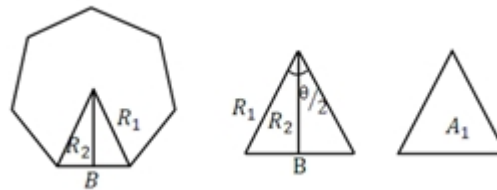


**Fig .(2) The geometry of heptagonal slot**

$$\theta = 360 / 7 = 51.428$$

$$R_2 = \cos(\theta / 2)R_1 \approx 0.9R_1 \quad \dots (1)$$

The area ( $A_1$ ) of the triangle shown in Figure 2 is therefore equal to:

$$A_1 = \frac{1}{2}B \times R_2 = \frac{1}{2}B \times 0.9R_1 = \frac{1}{2}0.7812R_1^2 = 0.391R_1^2$$

where  $B \approx 0.868R_1$  approximately in heptagon. The total area of the heptagonal structure is then equal to:

$$A = 7A_1 = 2.737R_1^2 \quad \dots (2)$$

In slot antenna, it is found that the lower edge frequency of the bandwidth can be approximately found by equating the area of the slot configuration to that of cylindrical wire [18]. By applying the same principle on the proposed heptagonal structure, we get:

$$2\pi rl = 2.737R_1^2 \dots\dots\dots (3)$$

where:

$r$ - the equivalent radius of the cylindrical wire.

$l$ - the height of the cylindrical wire.

$R_1$ - the main radius of the heptagonal slot.

The lower edge frequency ( $f_L$ ) of the bandwidth is given by [19]:

$$f_L(\text{GHz}) = \frac{c}{\lambda} = \frac{30 \times 0.32}{(l + r)}$$

or 
$$f_L(\text{GHz}) = \frac{9.6}{(R_1 + 0.4356R_1)} \dots\dots\dots (4)$$

The dimensions of  $l$ ,  $r$ ,  $R_1$  are all in centimeters.

In order to take the effect of substrate in consideration, the above equation can be modified as:

$$f_L(\text{GHz}) = \frac{9.6}{(R_1 + 0.4356R_1)\sqrt{\epsilon_{\text{reff}}}} \dots\dots\dots (5)$$

where  $\epsilon_{\text{reff}}$  is the effective relative permittivity of the substrate, and given by [20].

$$\epsilon_{\text{reff}} = \frac{\epsilon_r + 1}{2} \dots\dots\dots (6)$$

### 3. Antenna Parametric Study

The main radius ( $R_1$ ) of the heptagon slot can be calculated according to Equation 5 as 13.5mm. Therefore, the values of (B) and ( $R_2$ ) are calculated as 11.718mm and 12.15mm respectively.

The heptagonal slot with a radius ( $R_1$ ) and a 50Ω microstrip feed line are printed on opposite sides of the FR4 dielectric substrate. The width and length of the ground plane and dielectric substrate are denoted by ( $W$ ) and ( $L$ ) respectively. To achieve 50Ω impedance, the width of the microstrip feed line ( $w_f$ ) is calculated as 2.89mm. In order to enhance the matching between the microstrip feed line in the top layer of substrate and the heptagonal slot in the

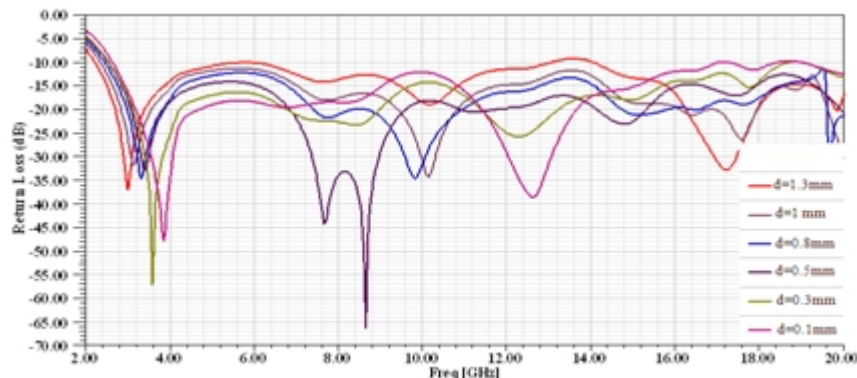
bottom of it, a rectangular tuning stub is used <sup>[21]</sup> with dimensions of ( $W_1 \times L_1$ ) which is notched cutting by rectangular with dimension ( $W_2 \times L_2$ ). The distance between the lower edge of heptagonal slot and the bottom of the tuning stub is denoted by ( $d$ ), the bevel angle of rectangular tuning stub is denoted by ( $\theta_1$ ), the slant angle cutting of the end of microstrip line is denoted by ( $\theta_2$ ), and the feed point position of the tuning stub is denoted by ( $x_1$ ).

The main parameters that affect the performance of the antenna are the electrical and geometrical parameters, such as slot dimensions in the ground plane, the distance between the bottom of tuning stub and lower edge of the slot, feed point position, bevel angle of rectangular tuning stub, and slant angle cutting off the end of the microstrip feed line.

In this section, the effect of important parameters on the performance of the antenna are analyzed and a parametric study is executed to optimize the antenna performance.

### 3.1. The distance between the bottom of tuning stub and lower edge of the heptagonal slot ( $d$ ):

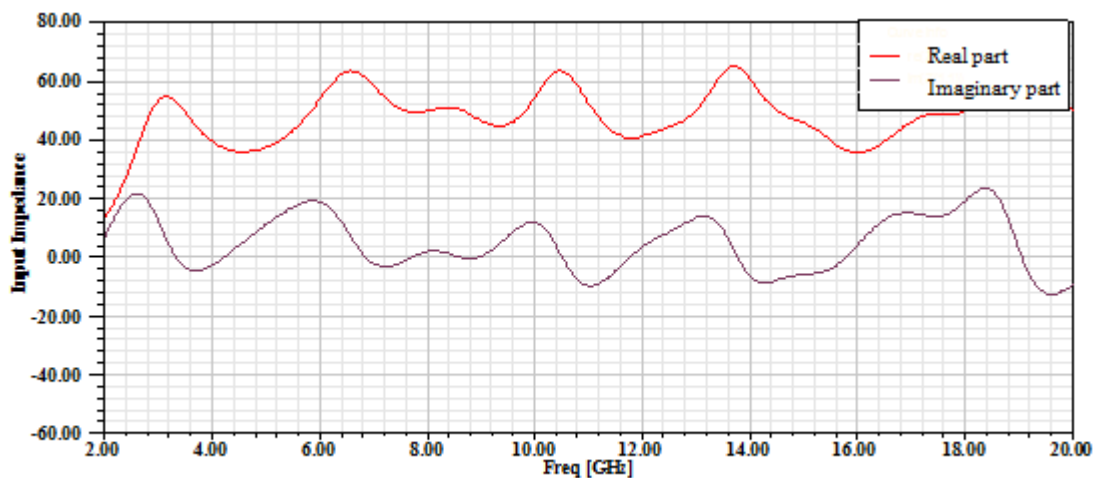
The first parameter to be optimized is the distance between the bottom of tuning stub at the top of dielectric substrate and lower edge of heptagonal slot at bottom of dielectric substrate ( $d$ ). The value of  $R_1$  is fixed at 13.5mm, and the other parameters are initially selected as  $L=40$ mm and  $W=30$ mm in order to just cover the heptagonal slot and the feed line, and also to give a bandwidth that covers the whole bandwidth according to FCC (3.1-10.6) GHz. **Figure (3)** and **Table 1** illustrated the -10dB bandwidth against the values of ( $d$ ). It is obvious that changing ( $d$ ) parameter has a significant effect on the -10dB bandwidth. This bandwidth becomes narrower as ( $d$ ) becomes larger since the impedance matching of the antenna becomes worse. It is also noticed that the return loss has approximately the same value (around 2.5GHz) for different values of  $d$ , which means that antenna response at the lower resonant frequency is not affected by the increasing of ( $d$ ). The optimum distance is thus found to be  $d=0.5$ mm. At this optimum value of  $d$ , the real part of the antenna input impedance shown in **Figure (4)** varies slowly around the  $50\Omega$  value, while the imaginary part of the antenna input impedance remains small across a wide frequency range, leading to a UWB performance.



**Figure 3: Simulated return loss of heptagonal slot antenna for different distances ( $d$ ) with  $R_1= 13.5$ mm,  $L= 40$ mm and  $W=30$ mm**

**Table .(1) Distance ( $d$ ) against the bandwidth of heptagonal slot antenna**

$d$ (mm)	Lower edge of bandwidth (GHz)	Upper edge of bandwidth (GHz)	Bandwidth (GHz)
0.1	2.64	17	14.36
0.3	2.56	18.8	16.24
0.5	2.53	More than 20	More than 17.47
0.8	2.45	More than 20	More than 17.55
1	2.35	More than 20	More than 17.65
1.3	2.22	13	10.78

**Fig .(4) Simulated input impedance of heptagonal slot antenna for  $d=0.5\text{mm}$  with  $R_f=13.5\text{mm}$ ,  $L=40\text{mm}$  and  $W=30\text{mm}$** 

### 3.2. Feed point position ( $x_f$ ):

The feed point position ( $x_f$ ) is the second parameter to be optimized keeping the values of  $R_f$ ,  $L$ , and  $W$  as in the previous section and  $d=0.5\text{mm}$ . **Figure (5)** shows the simulation return loss of the proposed antenna as a function of frequency. Many different values of feed point position ( $x_f$ ) are listed in **Table 2** against the bandwidth of proposed antenna. It is noticed that the impedance matching is getting worse as ( $x_f$ ) becomes very close to any slot side. The impedance matching increases when feed point is near the center of the lower edge of slot due to the symmetry of current distribution along the slot, and thus a larger bandwidth is obtained. The optimal value of the feed point position is found at  $x_f=20\text{mm}$ . The real and imaginary parts of the input impedance of proposed antenna are shown in **Figure (6)**. Both the resistance and reactance are fluctuating around  $50\Omega$  and  $0\Omega$  respectively, when the value of  $x_f$  is  $20\text{mm}$ , which leads to a wide operating bandwidth.

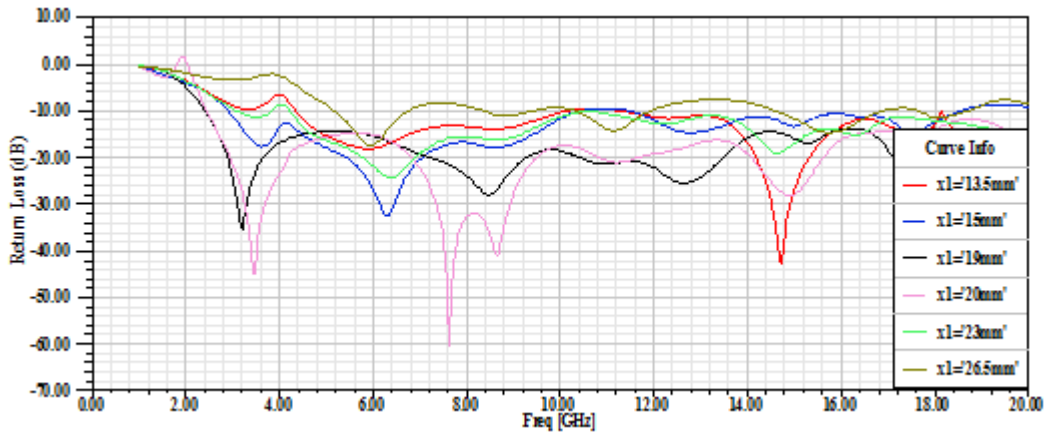


Fig .(5) Simulated return loss of heptagonal slot antenna for different feed point positions with  $R_f= 13.5\text{mm}$ ,  $L= 40\text{mm}$ ,  $d=0.5\text{mm}$  and  $W=30\text{mm}$

Table .(2) Feed point position ( $x_1$ ) against the bandwidth of heptagonal slot antenna

$x_1(\text{mm})$	Lower edge of bandwidth (GHz)	Upper edge of bandwidth (GHz)	Bandwidth (GHz)
13.5	4.35	10.18	Does not cover the whole UWB bandwidth
15	2.95	10.44	Does not cover the whole UWB bandwidth
19	2.41	More than 20	More than 17.59
20	2.44	More than 20	More than 17.56 but the response is better than $x_f=19\text{mm}$
23	3.09	3.83	Does not cover the whole UWB bandwidth
26.5	5.19	6.78	Does not cover the whole UWB bandwidth

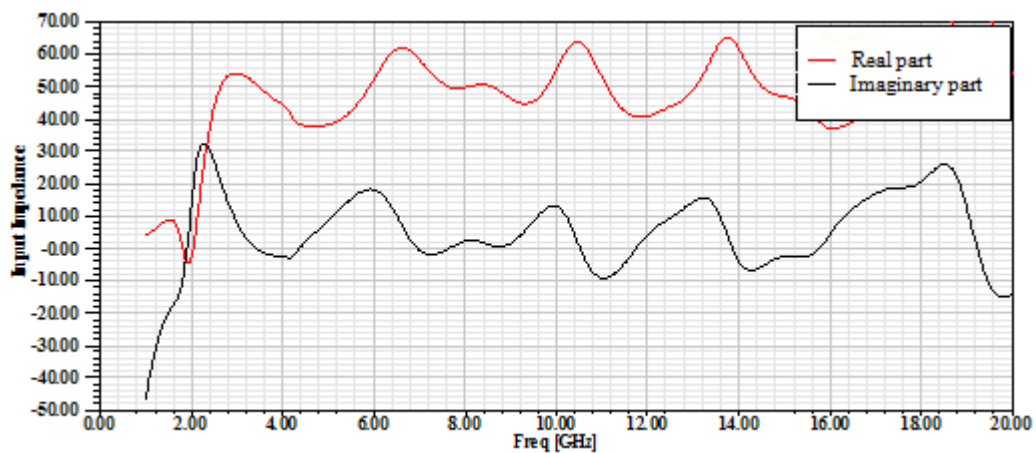


Fig .(6) Simulated input impedance of heptagonal slot antenna for feed point position  $x_f=20\text{mm}$  with  $R_f= 13.5\text{mm}$ ,  $L= 40\text{mm}$ ,  $d=0.5\text{mm}$  and  $W=30\text{mm}$

### 3.3. Ground Plane Width ( $W$ )

The third parameter to be optimized is the ground plane width using  $R_f=13.5\text{mm}$ ,  $L=40\text{mm}$ ,  $d=0.5\text{mm}$  and  $x_f=20\text{mm}$ . **Figure (7)** shows the simulated antenna return loss for different value of ground plane width ( $W$ ). **Table 3** shows the -10dB bandwidth of the antenna for different values of ( $W$ ). The influence of the ground plane width variation is clear through shifting all the resonance modes across the spectrum. It is apparent that the variation of ground plane width does not affect the response of proposed antenna since the current distribution is concentrated along the edge of heptagonal slot and feed line. The optimal value of ground plane width is found to be at  $W=40\text{mm}$ .

**Table .(3) Ground plane width ( $W$ ) against the bandwidth of heptagonal slot antenna**

$W(\text{mm})$	Lower edge of bandwidth (GHz)	Upper edge of bandwidth (GHz)	Bandwidth (GHz)
30	2.51	16.91	14.4
32	2.55	More than 20	More than 17.45
34	2.75	More than 20	More than 17.25
36	2.65	More than 20	More than 17.35
38	2.49	More than 20	More than 17.51
40	2.47	More than 20	More than 17.53

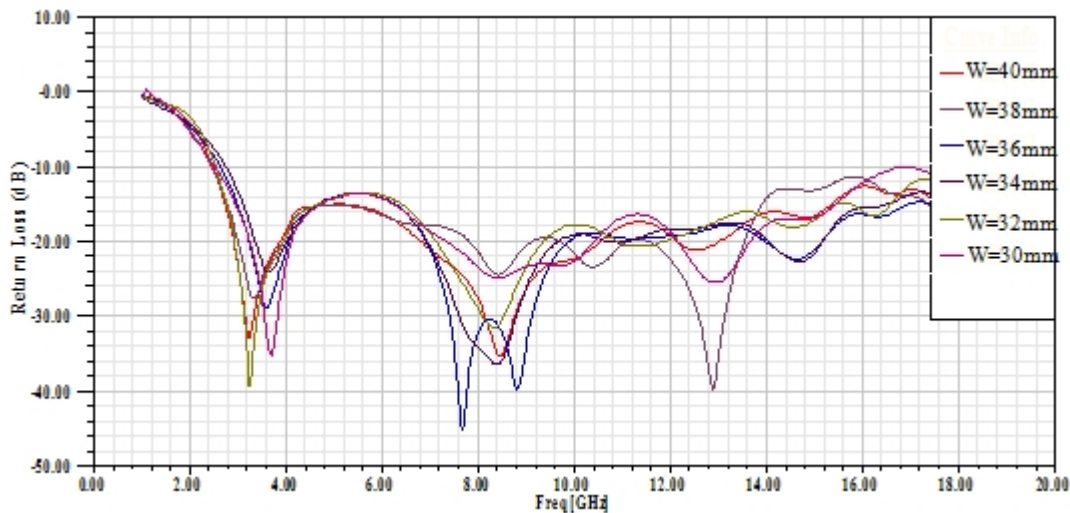


**Fig .(7) Simulated return loss of heptagonal slot antenna for different ground widths with feed point position  $x_f=20\text{mm}$ ,  $R_f= 13.5\text{mm}$ ,  $d=0.5\text{mm}$  and  $L=40\text{mm}$**



### 3.4. Ground Plane Length ( $L$ ):

The fourth parameter to be optimized is the ground plane length ( $L$ ) using  $R_1=13.5\text{mm}$ ,  $W=40\text{mm}$ ,  $d=0.5\text{mm}$  and  $x_1=20\text{mm}$ . The simulated antenna return loss as a function of frequency with different values of ground length ( $L$ ) is shown in Figure 8. It is clear that the antenna -10dB bandwidth is not affected very much by the variation of ( $L$ ). Since the current of the antenna is mainly distributed along the y-direction, therefore the ground plane length ( $L$ ) can be decreased without loss much of the bandwidth, leading to a procedure for miniaturization of the antenna size. The optimum value of  $L$  is found as 48mm.

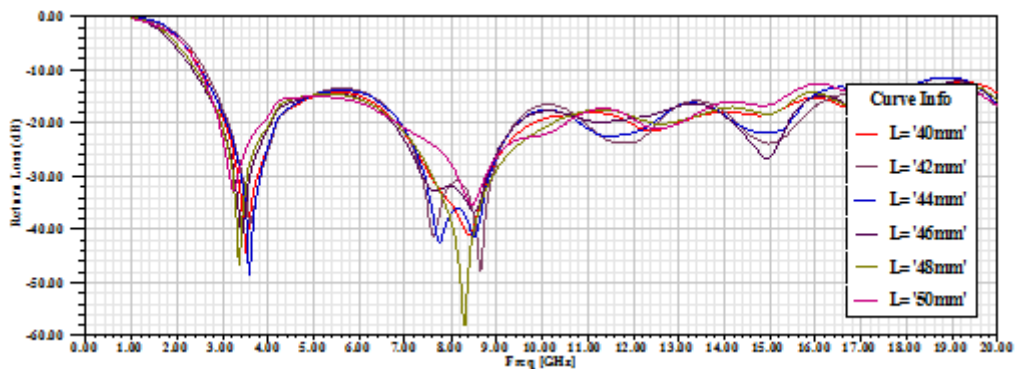


**Fig .(8) Simulated return loss of heptagonal slot antenna for different ground lengths with  $x_1=20\text{mm}$ ,  $R_1= 13.5\text{mm}$ ,  $W=40\text{mm}$  and  $d=0.5\text{mm}$**

### 3.5. Bevel angle $\theta_1$ :

The fifth parameter to be optimized is the bevel angle ( $\theta_1$ ) using  $R_1=13.5\text{mm}$ ,  $W=40\text{mm}$ ,  $d=0.5\text{mm}$ ,  $x_1=20\text{mm}$  and  $L=48\text{mm}$ . The simulated return loss of antenna versus the frequency for different values of the bevel angle ( $\theta_1$ ) is presented in Figure 9. It is clear that the values of bevel angle are affecting the matching impedance for the whole bandwidth, especially at high frequencies. Higher frequencies can be controlled and hence the entire band can be enhanced by adjusting the bevel angles. By varying the angle of the bevel ( $\theta_1$ ), the low and middle frequencies are highly influenced. Thus, using bevel provides more degrees of freedom and by adjusting this angle, the bandwidth will be widened as well as a good level of matching can be achieved. The optimum bevel angle is found to be at  $\theta_1 = 26^\circ$ .

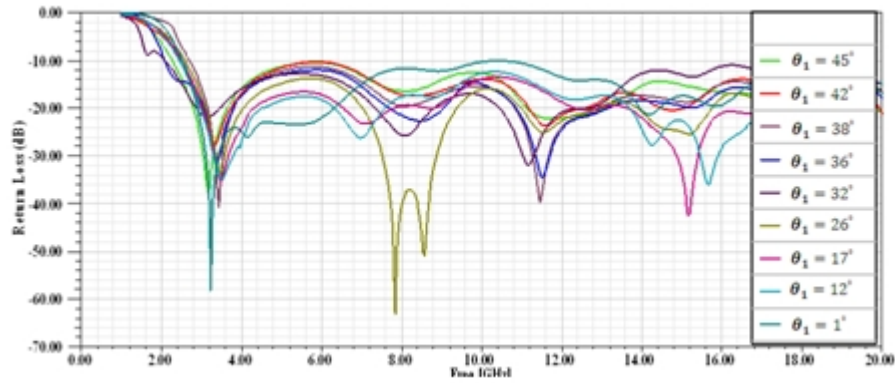


Fig .(9) Simulated return loss of heptagonal slot antenna for different bevel angles  $\theta_1$  with  $x_1=20\text{mm}$ ,  $R_1= 13.5\text{mm}$ ,  $W=40\text{mm}$ ,  $L=48\text{mm}$  and  $d=0.5\text{mm}$

### 3.6. Slant angle $\theta_2$ :

The sixth parameter to be optimized is the slant angle ( $\theta_2$ ) using  $R_1=13.5\text{mm}$ ,  $W=40\text{mm}$ ,  $d=0.5\text{mm}$ ,  $x_1=20\text{mm}$ ,  $L=48\text{mm}$  and  $\theta_1=26^\circ$ . The simulated return loss of proposed antenna with respect to the frequency for different values of the slant angle ( $\theta_2$ ) is plotted in Figure 10. It is observed that the lower frequency of the -10dB bandwidth is independent of the slant angle ( $\theta_2$ ), but higher frequencies of this bandwidth that are very sensitive to changing of the slant angle ( $\theta_2$ ). This is because the slant angle affects the coupling between the rectangular tuning stub and the ground plane. The optimum slant angle is found to be at  $\theta_2=13^\circ$ . Other important parameters which have some effects on the response of the proposed antenna are the dimensions of the rectangular tuning stub. These dimensions are optimized, and found as  $W_1=10\text{mm}$ ,  $L_1=10.8\text{mm}$ ,  $W_2=3.6\text{mm}$ ,  $L_2=8\text{mm}$ .

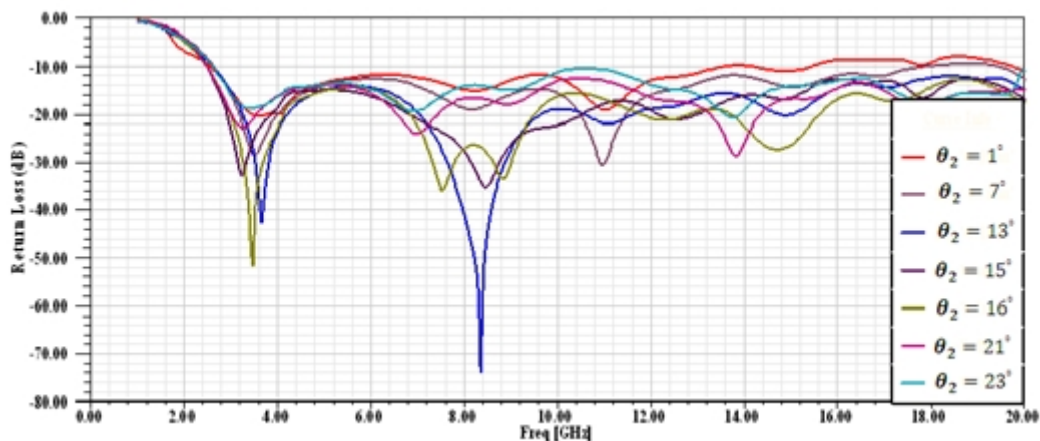
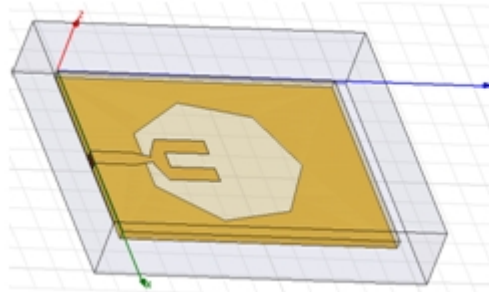


Fig .(10) Simulated return loss of heptagonal slot antenna for different slant angle  $\theta_2$  with  $x_1=20\text{mm}$ ,  $R_1= 13.5\text{mm}$ ,  $W=40\text{mm}$ ,  $L=48\text{mm}$ ,  $d=0.5\text{mm}$  and  $\theta_1=26^\circ$

#### 4. The Optimized Design

The optimized heptagonal slot antenna is constructed as shown in **Figure (11)** taking into account the final parameter values shown in **Table 4**.



**Fig .(11)** The prototype of the heptagonal slot antenna with  $R_1=13.5\text{mm}$ ,  $d=0.5\text{mm}$ ,  $W=40\text{mm}$ ,  $L=48\text{mm}$ ,  $W_1=10\text{mm}$ ,  $L_1=10.8\text{mm}$ ,  $W_2=3.6\text{mm}$ ,  $L_2=8\text{mm}$ ,  $x_1=20\text{mm}$ ,  $\theta_1 = 26^\circ$ , and  $\theta_2 = 13^\circ$

**Table .(4)** Optimal design parameters of heptagonal slot antenna

Parameter	Value
the substrate thickness ( $h$ )	1.5mm
relative permittivity ( $\epsilon_r$ )	4.4
the length of the substrate ( $L$ )	48mm
the width of the substrate ( $W$ )	40mm
the width of the rectangular tuning stub ( $W_1$ )	10mm
the length of the rectangular tuning stub ( $L_1$ )	10.8mm
the width of the rectangular notch cutting ( $W_2$ )	3.6mm
the length of the rectangular notch cutting ( $L_2$ )	8mm
the width of the microstrip feed line ( $W_f$ )	2.89mm
the distance ( $d$ )	0.5mm
bevel angle ( $\theta_1$ )	$26^\circ$
slant angle ( $\theta_2$ )	$13^\circ$

#### 5. Results And Discussion

The optimized antenna structure is first simulated at three different frequencies 3.5GHz, 7.5 GHz and 8.5 GHz. The resulted current distributions at these frequencies are presented in **Figure (12)**.

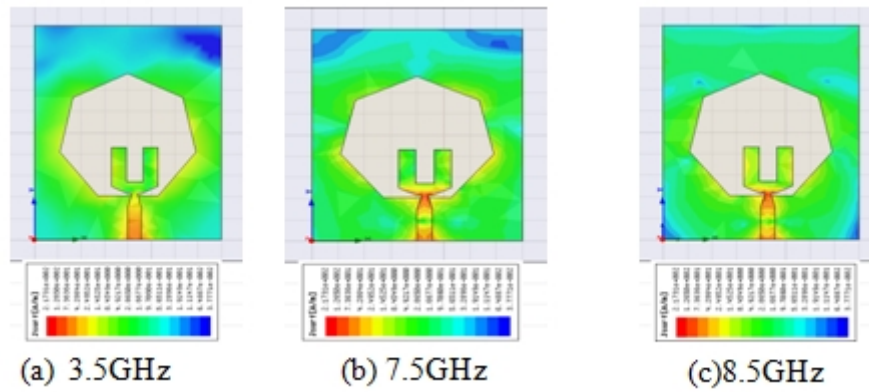


**Fig .(12) Simulated current distribution of the optimized heptagonal slot antenna for different resonance frequencies**

It is clear that the current distribution is mainly centralized along the edge of the heptagonal slot and the rectangular tuning stub, and this explains why the first resonant frequency is affected by the slot dimensions. The pattern of these frequencies indicates an existence of different resonance modes at different frequencies. This proves that the heptagonal slot antenna is qualified to support multi resonant modes, and the overlapping of these modes produced an UWB characteristic.

### 5.1. Return loss

**Figure (13)** shows the return loss of the optimized antenna. The -10dB bandwidth is found to remain under -10dB (2-20) GHz. Therefore, the bandwidth of the antenna is more than 18 GHz. It is clear that the optimized antenna supports multiple closely distributed resonance modes, as mentioned previously. Actually, the UWB characteristic of this antenna is resulted from the overlapping of these resonance modes.

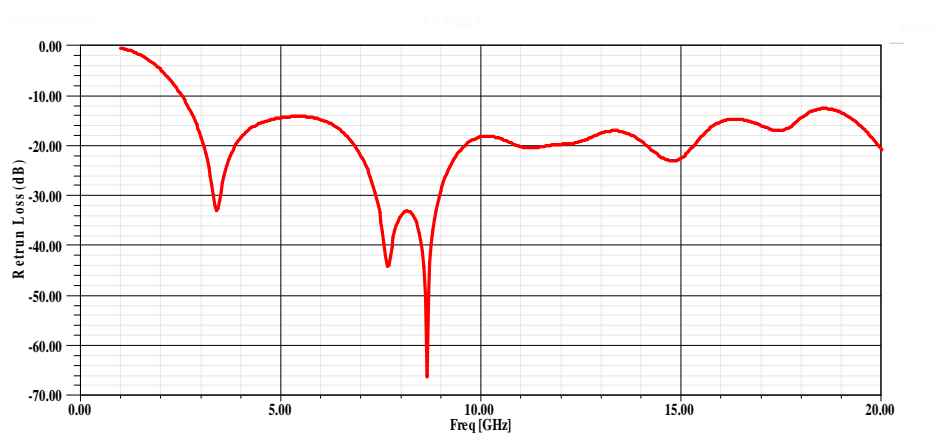


**Fig .(13) Return loss of the heptagonal slot antenna with optimum dimensions**

## 5.2. Radiation pattern

The E-plane and H-plane radiation patterns of the optimized antenna structure are shown in **Figure (14, 15 and 16)** at frequencies 3.5 GHz, 7.5 GHz and 8.5 GHz respectively. These radiation patterns show that the proposed antenna has omni-directional patterns (one of UWB properties) in the H-plane for all frequencies. The E-plane patterns, at low frequencies form a figure-of-eight patterns, with dips at high frequencies. The heptagonal slot antenna shows an acceptable radiation pattern variation in its entire operational bandwidth since the reduction happens only for a small part of the whole bandwidth and it is not too drastic.

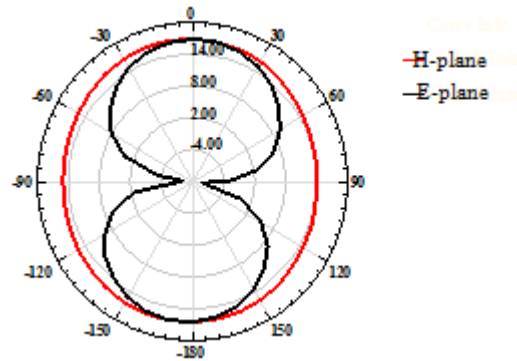


**Fig .(14)** The simulated H-plane and E-plane radiation patterns at 3.5GHz

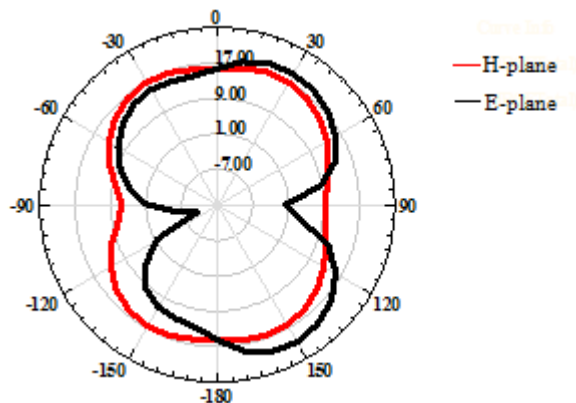


**Fig .(15)** The simulated H-plane and E-plane radiation patterns at 7.5GHz

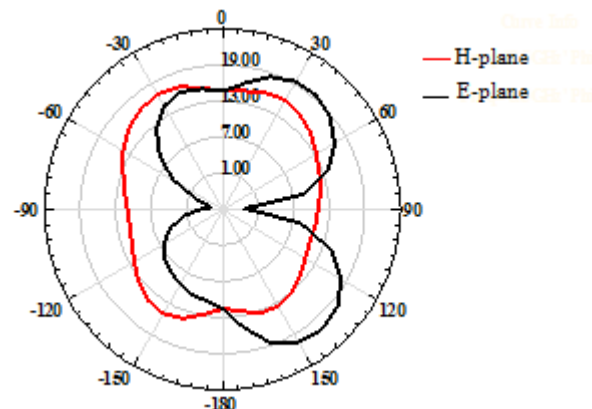


**Fig .(16)** The simulated H-plane and E-plane radiation patterns at 8.5GHz

### 5.3. Antenna gain

The antenna gain versus frequency plot is shown in **Figure (17)**. It is greater than 2.9 dB for all frequencies in the desired band and varies from 2.9 dB to 7.64 dB over the operating frequency range.

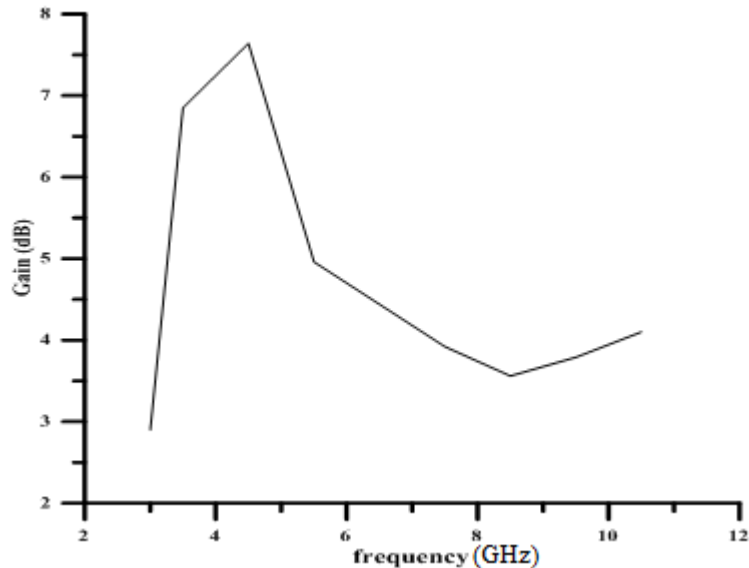


Fig .(17) The peak gain (dB) versus frequency

## 6. Time Domain Performance Of The Optimized Antenna

To find the transfer function, a system set up is used, as shown in **Figure (18)**, which is consisted of two identical heptagonal slot antennas at the transmitter and receiver. The transmitted and received antennas are vertically placed with a separation of 30cm, (the far field distance) <sup>[22]</sup>, so that they face each other.

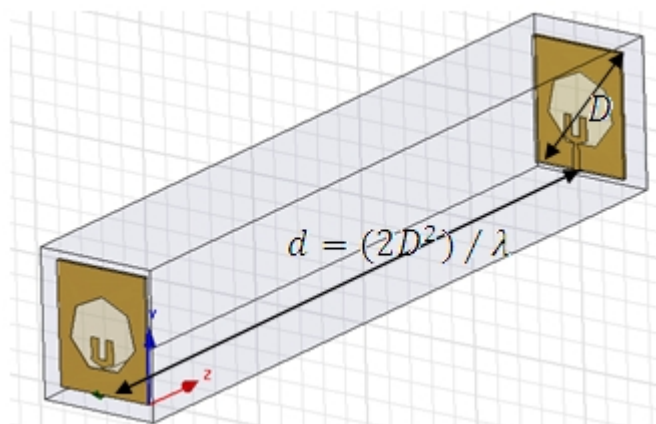


Fig .(18) System set up

## 6.1. Magnitude of Transfer Function

Figure (19) shows the magnitude of the transfer function of the heptagonal slot antenna pair. It is clear that the operating band, which is -10dB below the peak, is less than 7GHz. This means the signal within this band will be almost equally received. In the band between 7GHz-8GHz, the magnitude of the transfer function diminishes sharply, which causes a distorted received signal. For frequencies higher than 8GHz the frequency components would be received except components around the frequency 9.5 GHz which will be distorted.

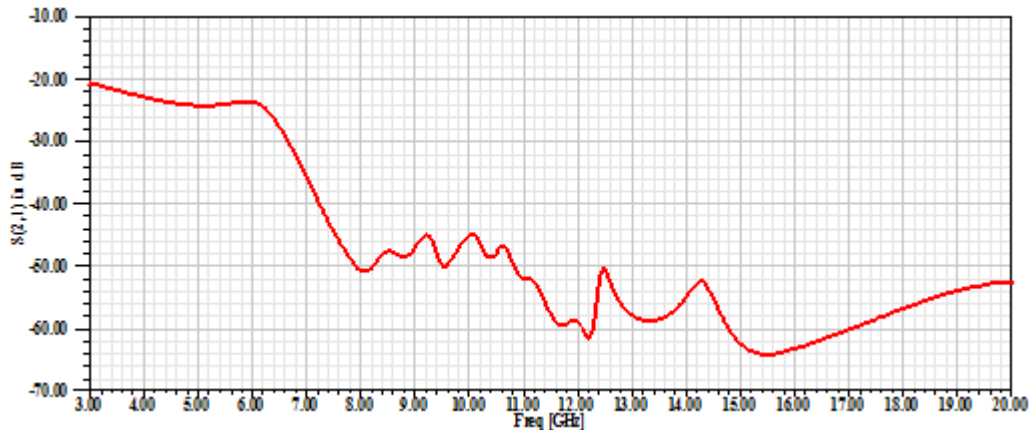


Fig .(19) Magnitude of transfer function of heptagonal slot antennas pair

## 6.2. Phase of Transfer Function

The phase of the transfer function of the heptagonal slot antenna pair is shown in Figure (20). It is clear that this response is nearly linear over the band 3GHz to 12.5 GHz.

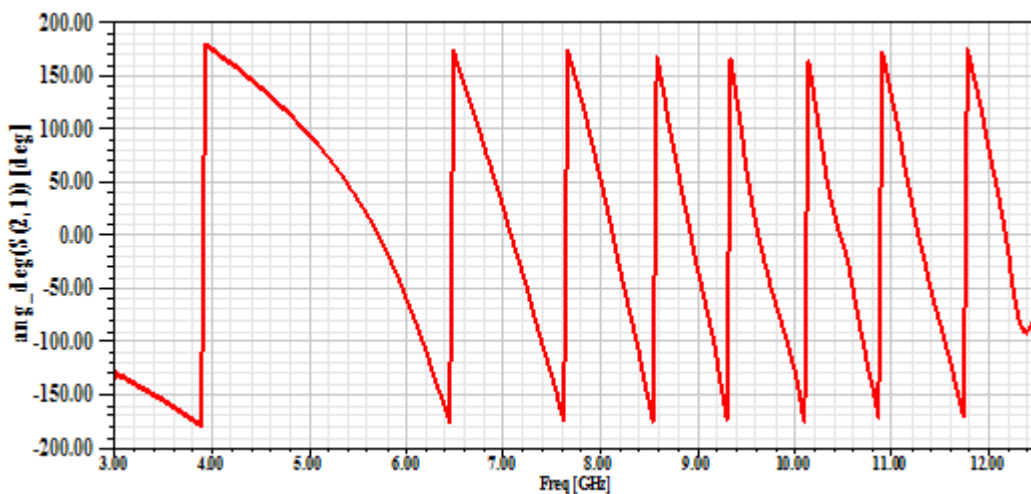
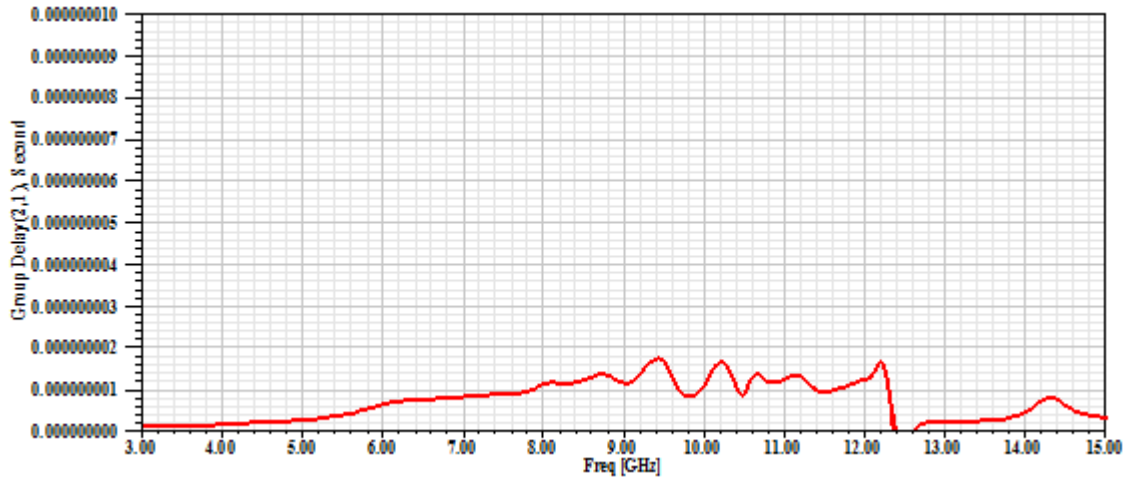


Fig .(20) Phase of transfer function of heptagonal slot antennas pair

### 6.3. Group Delay of Transfer Function

The group delay of the transfer function of the heptagonal slot antenna pair is shown in **Figure (21)**. This curve can be considered stable with variation less than 1.8ms in the band 3GHz to 12.3 GHz, which agrees well with the phase of the transfer functions.



**Fig .(21) Group delay of transfer function of heptagonal slot antenna pair**

## 7. Conclusion

A novel, small, low-profile heptagonal slot antenna is designed and analyzed in this paper to meet technology requirements. The proposed antenna consists of a heptagonal slot in the ground plane and a  $50\Omega$  microstrip feed line with rectangular tuning stub etched on the opposite sides of a dielectric substrate. This feed line is tapered at its end with certain slant angle  $\theta_2$  to widen bandwidth, and rectangular tuning stub to increase the matching between the slot and the feed line. Thus, the slot dimension, the distance  $d$ , bevel angle of rectangular tuning stub  $\theta_1$ , and slant angle  $\theta_2$  are the most important parameters that control the antenna performance.

The frequency domain characteristics of the antenna such as the radiation pattern, gain and impedance bandwidth are found acceptable in the entire operational bandwidth. The proposed antenna operates as omni-directional radiation properties over a major fraction of the bandwidth. The time domain characteristics of the antenna also found acceptable and the antenna proved to possess linear phase over the operational bandwidth, which leads to constant group delay and less distortion of the received signal.



## References

1. First Report and Order, "Revision of Part 15 of the Commission's Rules Regarding Ultra-wideband Transmission Systems Federal Communication Commission FCC, 02-48", April 22, 2002.
2. Schantz, H. G., "UWB Magnetic Antennas", IEEE Antennas and Propagation Society International Symposium, Vol. 3, June 2003, pp. 604-607.
3. Mandal, T., and S. Das, "a coplanar waveguide fed ultra wideband hexagonal slot antenna with dual band rejection", Progress In Electromagnetics Research C, Vol. 39, 209-224, 2013.
4. Chiou, J., Y., J. Y. Sze and K. L. Wong, "A Broad-Band CPW-Fed Strip-Loaded Square Slot Antenna", IEEE Transactions on Antennas and Propagation, Vol. 51, No. 4, April 2003, pp. 719-721.
5. Jang, Y., W. "Broadband Cross-shaped Microstrip-Fed Slot Antenna", Electronics Letters, Vol. 36, No. 25, December 2000, pp. 2056-2057.
6. Myung, K., K., K. Kim, Y. H. Suh and I. Park, "A T-Shaped Microstrip-Line-Fed Wide Slot Antenna", IEEE Antennas and Propagation Society International Symposium, July 2000, pp. 1500-1503.
7. Gino, S., F. Consoli and S. Barbarino, "Numerical and experimental analysis of a circular slot antenna for UWB communications", Microwave and Optical Technology Letters, Vol. 44, No. 5, March 5 2005, pp. 465-470.
8. Soliman, E., A., S. Brebels, E. Beyne and G. A. E. Vandebosch, "CPW-fed cusp antenna", Microwave and Optical Technology Letters, Vol. 22, No. 4, August 20 1999, pp. 288-290.
9. Liu, Y., F., K. L. Lau, Q. Xue and C. H. Chan, "Experimental studies of printed wide-slot antenna for wide-band applications", IEEE Antennas and Wireless Propagation Letters, Vol. 3, 2004, pp. 273-275.
10. Chen W., S., and F. M. Hsieh, "Broadband design of the printed triangular slot antenna", IEEE Antennas and Propagation Society International Symposium, vol. 4, 20-25 June 2004, pp. 3733 - 3736.
11. Chen, J. S., "Dual-frequency annular-ring slot antennas fed by CPW feed and microstrip line feed", IEEE Transactions on Antennas and Propagation, Vol. 53, No. 1, January 2005, pp. 569-571.
12. Yeo, J., Y. Lee and R. Mittra, "Wideband slot antennas for wireless communications", IEE Proceedings of Microwaves, Antennas & Propagation, Vol. 151, No. 4, August 2004, pp. 351-355.
13. Chen, W., S., Ch. Ch. Huang and K. L. Wong, "A novel microstrip-line-fed printed semicircular slot antenna for broadband operation", Microwave and Optical Technology Letters, Vol. 26, No. 4, August 20 2000, pp. 237-239.

14. Lee, H., L., J. G. Yook and H. K. Park, "Broadband planar antenna having round corner rectangular wide slot", IEEE Antennas and Propagation Society International Symposium, Vol. 2, 16-21 June 2002, pp. 460-463.
15. Sze, J., Y., and K. L. Wong, "Bandwidth Enhancement of a Microstrip -Line-Fed Printed Wide-Slot Antenna", IEEE Transactions on Antennas and Propagation, Vol. 49, No. 7, July 2001, pp. 1020-1024.
16. Chen, H., D., "Broadband CPW-fed Square Slot Antennas with A Widened Tuning Stub", IEEE Transactions on Antennas and Propagation, Vol. 51, No. 8, August 2003, pp. 1982-1986.
17. Chair, R., A. A. Kishk and K. F. Lee, "Ultrawide-band Coplanar Waveguide-Fed Rectangular Slot Antenna", IEEE Antenna and Wireless Propagation Letter, Vol.3, No. 12, 2004, pp. 227-229.
18. Agrawall, N., P., G. Kumar, and K. P. Ray, "Wide-Band Planar Monopole Antennas", IEEE Transactions on Antennas and Propagation, Vol. 46, No. 2, February 1998, pp. 294-295.
19. Pengcheng, L., J. Liang, and X. Chen, "Study of Printed Elliptical/Circular Slot Antennas for Ultrawideband Applications", IEEE Transactions on Antennas and Propagation, Vol. 54, No. 6, June 2006, pp. 1670-1675
20. Guihong, L., H. Zhai, T. Li, X. Ma, and Ch. Liang, "Design of a Compact UWB Antenna Integrated with GSM/WCDMA/WLAN bands," Progress In Electromagnetics Research, Vol. 136, 409-419, 2013.
21. Song, K., Y. Z. Yin, S.T. Fan, and B. Chen, "compact open-ended l-shaped slot antenna with asymmetrical rectangular patch for UWB applications," Progress In Electromagnetics Research C, Vol. 19, 235-243, 2011.
22. Balanis, C., A., "Antenna Theory Analysis and Design," 2005, John Wiley & Sons, INC., 2005.